Eur. Phys. J. B **51**, 245–255 (2006)
DOI: 10.1140/epjb/e2006-00217-7

THE EUROPEAN PHYSICAL JOURNAL B

Nonequilibrium critical behavior of a species coexistence model

H. Reinhardt[1], F. Böhm[1], B. Drossel[1,a], and H. Hinrichsen[2,b]

[1] Institut für Festkörperphysik, TU Darmstadt, Hochschulstraße 6, 64289 Darmstadt, Germany
[2] Fakultät für Physik und Astronomie, Universität Würzburg, Am Hubland, 97074 Würzburg, Germany

Received 10 March 2006 / Received in final form 11 April 2006
Published online 2 June 2006 –

Abstract. A biologically motivated model for spatio-temporal coexistence of two competing species is studied by mean-field theory and numerical simulations. In $d \geq 2$ dimensions the phase diagram displays an extended region where both species coexist, bounded by two second-order phase transition lines belonging to the directed percolation universality class. The two transition lines meet in a multicritical point, where a non-trivial critical behavior is observed.

PACS. 87.23.Cc Population dynamics and ecological pattern formation – 05.70.Ln Nonequilibrium and irreversible thermodynamics – 64.60.Ak Renormalization-group, fractal, and percolation studies of phase transitions

1 Introduction

Nonequilibrium models with phase transitions into absorbing states arise in studies of biological populations, chemical reactions, spreading of diseases, and many other [1–5]. An absorbing phase is a subspace of states that can be reached but not be left by the dynamics. In biologically motivated models absorbing phases occur whenever a system reaches a configuration or a dynamical state from where it cannot escape. In many cases an absorbing state is characterized by a complete loss of activity. It is believed that phase transitions into an absorbing state generically belong to the directed percolation (DP) universality class [6–8]. DP is extremely robust and includes even models with several species of particles [9–11] and infinitely many absorbing states [12,13]. Exceptions from DP are usually observed in models with long-range interactions, quenched randomness, and non-conventional symmetries such as a Z_2-symmetry or conservation of particle number.

In models with several species of particles and several absorbing states, there exist in addition to transitions where one species goes extinct, multicritical points where several reduced control parameters vanish simultaneously. Such multicritical points are characterized by a hierarchy of order parameter exponents with only one of them being the DP exponent, and by a crossover exponent ϕ [14,15]. Again, the multicritical behavior is different in the presence of symmetries [16].

Most DP models have in common that active sites may become inactive at a certain rate, i.e. particles can disappear spontaneously. But even models with a different mechanism for particle removal may belong to the DP class. For example, in branching and annihilating random walks particles can only annihilate pairwise, leading to an algebraic decay in the subcritical phase. Until recently, it was believed that such models do not show a DP-like phase transition in dimensions larger than two. However, as has been shown by Canet et al. [17], in higher dimensions such transitions occur also, but only beyond a minimum annihilation rate, so that freshly produced offspring can annihilate with its parent with a sufficiently large probability before diffusing away.

In this article, we consider a two-species model, which is inspired by biology. A special feature of this model is that one of the two species (denoted as S) cannot vanish spontaneously, instead it can only be destroyed by the other one (called A). In one dimension it turns out that the two species cannot coexist and the phase transition is discontinuous for the first species. In higher dimensions the two species can coexist in a certain region of the phase diagram, giving rise to three different phases. We find numerically that all phase boundaries where one species becomes extinct, are in the DP class, while the multicritical point where the two critical lines meet, shows a more complex scaling behavior. Near the multicritical point, the critical region becomes very small, and therefore the DP behavior can hardly be seen in numerical simulations. We apply numerical studies as well as mean-field calculations and scaling arguments. In addition to the stationary state, we also investigate the dynamical behavior starting from a random initial state. We find that two different scaling forms are needed to describe different dynamical regimes.

The outline of this paper is as follows: in the next section, we motivate and define our model. In Section 3 we formulate a mean field theory and discuss the corresponding phase diagram. Numerical simulations in one and two

[a] e-mail: barbara.drossel@physik.tu-darmstadt.de
[b] e-mail: hinrichsen@physik.uni-wuerzburg.de

spatial dimensions are presented in Section 4. In Section 5 we suggest a phenomenological scaling theory for the dynamical and the stationary regimes. Finally, we summarize our findings in Section 6.

2 Definition and motivation of the model

The model is defined on a d-dimensional hypercubic lattice with L^d sites. Each lattice site is occupied either by species A, or by species S, or it is empty. The system evolves random-sequentially according to the following dynamic rules:

- any site that has a nearest neighbor occupied by species A becomes itself occupied by species A with rate λ_A, irrespective of its previous state;
- an empty site that has a nearest neighbor occupied by species S becomes itself occupied by species S with rate λ_S;
- a site occupied by species A turns into an empty site with rate μ.

This means that the model follows the reaction-diffusion scheme

$$A + \emptyset \xrightarrow{\lambda_A} 2A, \qquad A \xrightarrow{\mu} \emptyset, \tag{1}$$
$$A + S \xrightarrow{\lambda_A} 2A, \qquad S + \emptyset \xrightarrow{\lambda_S} 2S.$$

The model can be considered as a patch occupancy model for the coexistence of two consumer species feeding on the same resources. The two species cannot coexist in the same patch, and therefore each patch is occupied at most by one of the two species [18]. Species A has the higher fitness and therefore displaces species S when it enters a patch occupied by S. However, species A has a certain risk of dying out in a patch, for instance because it cannot respond well to adverse circumstances, such as illness or extreme weather conditions. A and S may stand for an asexual and a sexual species, for instance oribatid mites in the soil [19], or ostracods in ponds lakes [20], where asexual and sexual species are known to have coexisted for a long time. Asexual species have a higher reproduction rate, but can accumulate deleterious mutations [21], which reduce their fitness below that of the sexual variant.

In our model the dynamics of species A is not affected by the presence of S since empty sites and sites occupied by S can both be conquered by A. The dynamics of species A is therefore a version of DP, and the phase transition of species A to extinction is in the DP universality class. More specifically, the dynamic rules of the A's are equivalent to those of a so-called contact process [22], which is a well-studied lattice model of DP with random-sequential updates. Precise estimates of the percolation threshold $\lambda_A^{(c)}/\mu$ [23–25] and the critical exponents [5] can be found in the literature and are summarized in Table 1.

In absence of species A, species S spreads and eventually occupies the entire system. In presence of species A patches of species S can only be destroyed if they are invaded by species A. Since the distribution of A is not homogeneous but highly correlated, patches occupied by S are not destroyed randomly, and it is not obvious that the phase transition to extinction of S has to be in the universality class of directed percolation. We will see below that this is nevertheless the case in dimensions larger than one, although the DP behavior is difficult to see when the density of A is low.

Table 1. Critical percolation thresholds $\lambda_A^{(c)}/\mu$ of the contact process of A-particles and the corresponding critical exponents of DP in d+1 dimensions.

d	$\lambda_A^{(c)}/\mu$	β	$\nu_\perp$	$\nu_\parallel$
1	1.648924(11)	0.276486(8)	1.096854(4)	1.733847(6)
2	0.41219(1)	0.583(3)	0.733(8)	1.295(6)
3	0.219477(2)	0.813(9)	0.584(5)	1.110(1)
4	0.14938(2)	1	1/2	1

Table 2. Fixed points of the mean-field equations (2, 3) and the corresponding conditions for stability.

F. point	ρ_A	ρ_S	conditions for stability	
F_1	0	0	$\lambda_S < 0$	$\lambda_A < \mu$
F_2	0	1	$\lambda_S > 0$	$\lambda_A < \mu$
F_3	$1 - \frac{\mu}{\lambda_A}$	0	$\lambda_S < \frac{\lambda_A^2}{\mu} - \lambda_A$	$\lambda_A > \mu$
F_4	$1 - \frac{\mu}{\lambda_A}$	$\frac{\mu}{\lambda_A} + \frac{\mu - \lambda_A}{\lambda_S}$	$\lambda_S > \frac{\lambda_A^2}{\mu} - \lambda_A$	$\lambda_A > \mu$

3 Mean field theory

Let us first discuss the mean-field theory of the model. The mean-field equations for the densities of species A and S are

$$\dot\rho_A(t) = \lambda_A \rho_A(t)\big[1 - \rho_A(t)\big] - \mu\rho_A(t), \tag{2}$$
$$\dot\rho_S(t) = \lambda_S \rho_S(t)\big[1 - \rho_A(t) - \rho_S(t)\big] - \lambda_A \rho_S(t)\rho_A(t). \tag{3}$$

The mean-field approximation can be viewed as the case where the A or S can move to any patch of the lattice with a given rate λ_A/L^d or λ_S/L^d, and not only to nearest neighbors, in the limit of infinite system size $L \to \infty$.

3.1 Stationary case

In order to determine the mean-field phase diagram we computed the stationary solutions of equations (2, 3). Table 2 lists the fixed points and the corresponding stationary densities ρ_A and ρ_S together with the conditions for their stability. The fixed point F_1 is unstable since λ_S and λ_A cannot be negative. The other three fixed points are stable in different parts of parameter space.

In the phase diagram the three fixed points correspond to three different phases (see Fig. 1). In the subcritical phase (marked by **S**) species A dies out so that species S eventually conquers the whole system, approaching the stationary density $\rho_S = 1$. In the coexistence phase

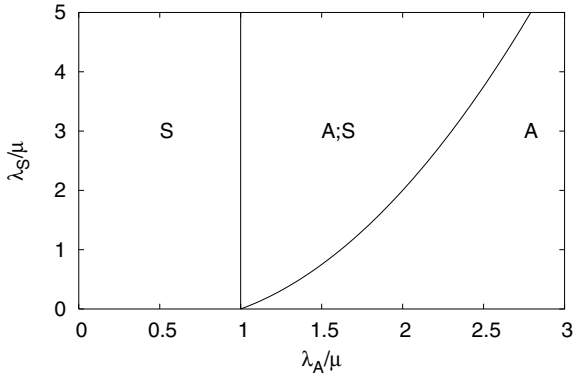

Fig. 1. Mean-field phase diagram. In phase **S** species A dies out so that species S conquers the whole system, while in phase **A** species S dies out. In phase **A;S** both species coexist, leading to a non-trivial fluctuating stationary state.

(marked by **A;S**) both species can coexist, leading to a non-trivial fluctuating stationary state with the densities

$$\rho_A = 1 - \frac{\mu}{\lambda_A}, \tag{4}$$

$$\rho_S = \frac{\mu}{\lambda_A} + \frac{\mu - \lambda_A}{\lambda_S}. \tag{5}$$

Finally, in the phase denoted by **A** in Figure 1, the density of species A is so high that species S becomes extinct. Here equation (4) is still valid while $\rho_S = 0$.

The three phases are separated by two lines of continuous phase transitions, a vertical one at $\lambda_A/\mu = 1$ and a curved one in form of a segment of a parabola

$$\lambda_S^* = \lambda_A^* \left(\frac{\lambda_A^*}{\mu} - 1 \right). \tag{6}$$

Approaching the vertical line from right to left the stationary density ρ_A vanishes linearly. The critical exponent β is therefore 1, just as in the standard mean-field theory of directed percolation. The same applies to the density ρ_S approaching the curved phase transition line from the left. This supports our numerical findings (see below) that both lines represent DP transitions.

The two phase transition lines meet at the multicritical point $\lambda_A/\mu = 1$; $\lambda_S = 0$. In order to discuss the behavior in the neighborhood of the multicritical point in more detail, it is convenient to introduce the parameters

$$\epsilon_A = \lambda_A/\mu - 1, \qquad \epsilon_S = \lambda_S/\mu, \tag{7}$$

which measure the reduced distances from the multicritical point in horizontal and vertical direction, respectively. In terms of these parameters the curved transition line (6) is given by

$$\epsilon_S^* = \epsilon_A^*(1 + \epsilon_A^*). \tag{8}$$

Close to the multicritical point, where both parameters are small, the densities scale as

$$\rho_A = 1 - \frac{1}{1+\epsilon_A} \simeq \epsilon_A, \tag{9}$$

$$\rho_S = \frac{1}{1+\epsilon_A} - \frac{\epsilon_A}{\epsilon_S} \simeq 1 - \frac{\epsilon_A}{\epsilon_S}. \tag{10}$$

As we decrease ϵ_A from ϵ_S to 0, we move horizontally from the curved to the vertical transition line, and ρ_S increases linearly from 0 to 1. Similarly, as we increase ϵ_S from ϵ_A to a value much larger than ϵ_A, we move from the curved transition line vertically upwards, and ρ_S increases from 0 to a value close to 1. Denoting by

$$\Delta_A = \epsilon_A^* - \epsilon_A \ \text{ and } \ \Delta_S = \epsilon_S - \epsilon_S^* \tag{11}$$

the horizontal and vertical distances between a given point (ϵ_A, ϵ_S) and the curved transition line, we have for $\Delta_A \ll \epsilon_A, \Delta_S \ll \epsilon_S$

$$\rho_S = \frac{\Delta_A}{\epsilon_S} = \frac{\Delta_S}{\epsilon_A}. \tag{12}$$

Therefore, the linear decrease of ρ_S does not depend on the direction in which the curved phase transition line is approached. However, the *slope* increases and finally diverges as we approach the multicritical point. This indicates that the transition with respect to S *at* the multicritical point may no longer belong to the DP class.

3.2 Time-dependent mean field solution

In order to understand the dynamical properties, let us now solve the time-dependent mean field equations (2, 3) explicitely. Since species A evolves independently according to the rules of DP equation (2) is autonomous. With $\epsilon_A = \lambda_A/\mu - 1$ and $\epsilon_S = \lambda_S/\mu$ the solution (up to a shift in time) reads

$$\rho_A(t) = \frac{\epsilon_A}{(1+\epsilon_A)\left[1 - \exp(-\epsilon_A \mu t)\right]}. \tag{13}$$

Close to criticality in the active phase $0 < \epsilon_A \ll 1$ this density first decays as a power law

$$\rho_A(t) \simeq \frac{1}{(1+\epsilon_A)\,\mu t} \tag{14}$$

until it crosses over to the stationary value given in equation (9) at some typical crossover time $t_c \sim \frac{1}{\mu \epsilon_A}$.

Inserting the solution (13) into the second mean field equation (3), it is in principle possible to compute the time-dependent density $\rho_S(t)$.

Let us first consider the case $\epsilon_A = 0$ (the vertical line in Fig. 1), where the DP process of species A is critical. Inserting equation (14) into equation (3), the second mean field equation reduces to

$$\dot\rho_S(t) \ = \ -\frac{\rho_S(t)}{t}\Big[1 + \epsilon_S + \epsilon_S \mu t \left(\rho_S(t) - 1\right)\Big]. \tag{15}$$

At the multicritical point $\epsilon_S = \epsilon_A = 0$ this differential equation further reduces to $\dot\rho_S(t) = -t^{-1}\rho_S(t)$ so that the density $\rho_S(t) \sim 1/t$ decays in the same way as $\rho_A(t)$. For $\epsilon_S > 0$, however, we find the formal solution

$$\rho_S(t) = \frac{\exp(\epsilon_S \mu t)}{(\epsilon_s \mu t)^{1+\epsilon_S}\left[C + \int_1^{\epsilon_S \mu t} e^z\, z^{-1-\epsilon_s}\, \mathrm{d}z\right]}, \tag{16}$$

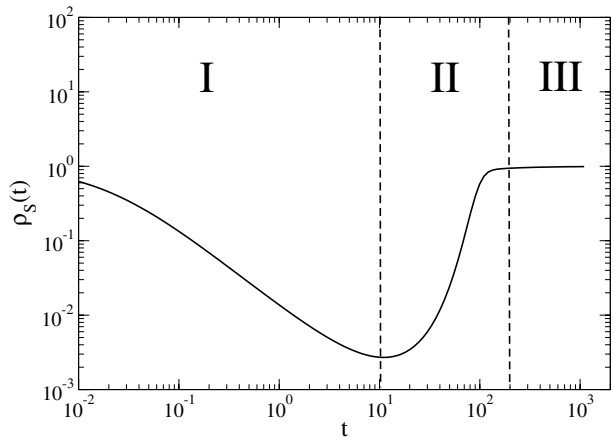

Fig. 2. Temporal evolution of the density $\rho_S(t)$ according to the mean-field solution (16) for $\epsilon_A = 0$, $\epsilon_S = 0.1$, $\mu = 1$ and $c = 10^3$. The three regimes are explained in the text.

where C is an integration constant. To get an impression about the behavior for $\epsilon_S > 0$, we plotted this function in Figure 2. As can be seen, there are three different dynamical regimes enumerated by I, II, and III. In the first regime the density $\rho_S(t)$ decreases algebraically as $1/t^{1+\epsilon_S}$, followed by a quick increase in the second regime until the density saturates at 1 in regime III.

The observed behavior can be interpreted as follows. Starting with a homogeneously distributed mixture of species A and S, the displacement of S by A initially dominates the dynamics. In regime II the spreading of S to empty patches, as expressed by the linear term $\lambda_S \rho_S(t)$ on the r.h.s. of equation (3), becomes relevant so that the S-population begins to grow exponentially in the voids of the critical A-process. The growth of the S-population continues until all accessible voids are filled and the density $\rho_S(t)$ reaches its stationary maximum in regime III.

Next, let us consider the dynamics on the curved phase transition line close to the multicritical point. Using equations (8) and (13), expanding ϵ_S and ρ_A in powers of ϵ_A and keeping only terms up to the third order in the densities and/or the control parameter, equation (3) turns into

$$\frac{1}{\mu}\,\dot{\rho}_S(t) = -\frac{\epsilon_A(1+\epsilon_A)}{\exp(\epsilon_A \mu t) - 1}\rho_S(t) - \epsilon_A \rho_S^2(t). \qquad (17)$$

The solution is

$$\rho_S(t) = \frac{[1 - \exp(-\epsilon_A \mu t)]^{-1-\epsilon_A}}{\tilde{C} + \int_1^{\epsilon_A \mu t} (1 - e^{-z})^{-1-\epsilon_A}\, \mathrm{d}z} \qquad (18)$$

with an integration constant $\tilde{C}$. This is a monotonous decay of the density ρ_S. For short times, it is approximated by $\rho_S \sim 1/t$, as we have obtained before. For large times, the density ρ_S approaches the behavior $\rho_S \simeq 1/\epsilon_A \mu t$, i.e., the decay is delayed. This large-time behavior is independent of the initial value of ρ_A, and it would therefore also be obtained if we had started with the stationary solution for ρ_A.

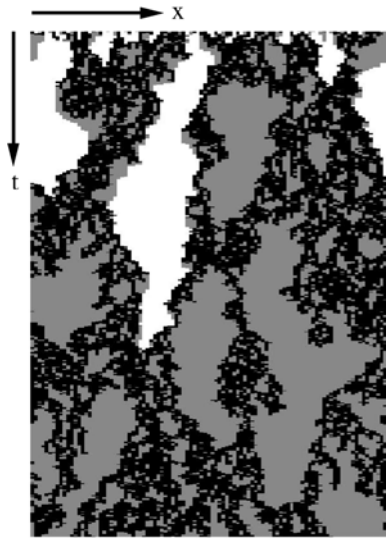

Fig. 3. Space-time plot of the 1+1-dimensional model. White and black sites correspond to species S and A respectively, and grey sites correspond to empty patches.

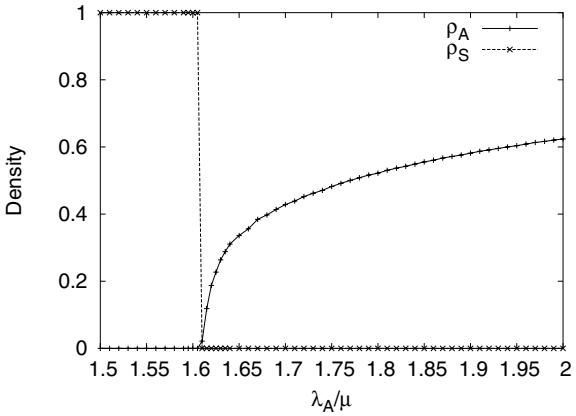

Fig. 4. Stationary density as a function of the control parameter λ/μ in one dimension (here $\lambda = \lambda_A = \lambda_S$).

4 Numerical simulations

4.1 Simulations in 1+1 dimensions

The 1+1-dimensional case is special in so far as species A and species S cannot coexist since the world lines of A and S cannot cross each other. Hence a species that persists forever leaves no room for a world line of the other species. Figure 3 shows a space-time plot of A, S and empty sites in the parameter range where A persists. As can be seen, starting from a random initial state, species S eventually dies out.

The stationary densities for A and S as functions of the control parameter λ_A/μ were measured in numerical simulations using a system size of $L = 50\,000$ sites. As shown in Figure 4, species S undergoes a first-order phase transition from unit density to zero density at the critical point $\lambda_A^{(c)}$ of species A.

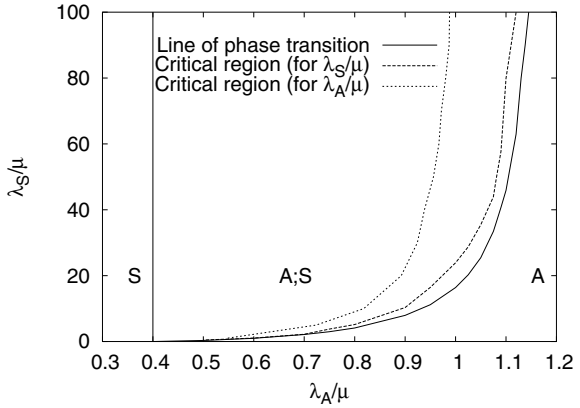

Fig. 5. Numerically determined phase diagram in 2+1 dimensions. The dotted lines denote the size of the critical regions for variation of λ_A/μ(dotted line) and λ_S/μ (dashed line).

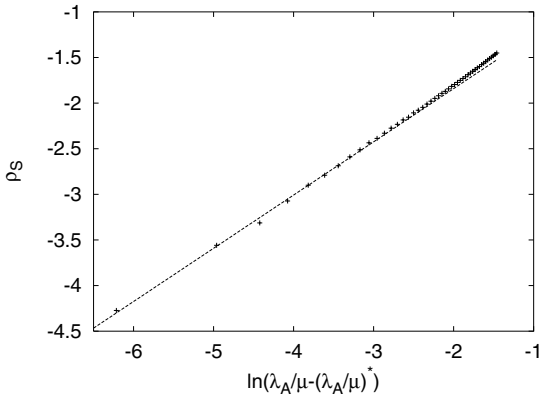

Fig. 6. Logarithmic plot of the stationary density ρ_S for $\lambda_S/\mu = 60$ as λ_A/μ is varied. A power-law fit in the interval $|\lambda_A/\mu - (\lambda_A/\mu)|^* <= 0.05$ yields the estimate $\beta_S = 0.583(3)$.

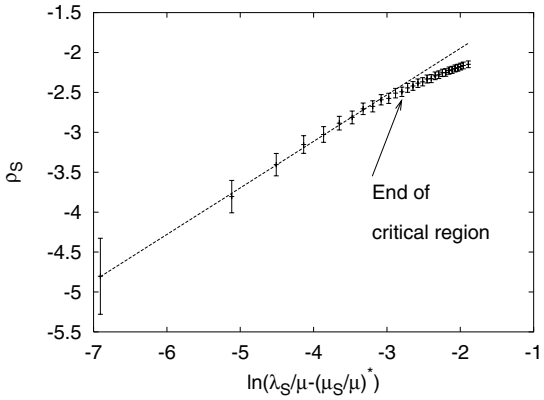

Fig. 7. Logarithmic plot of ρ_S, including its fluctuations for $\lambda_A/\mu = 1$. The power-law fit gives the exponent $\beta = 0.584(9)$.

4.2 Stationary properties in 2+1 dimensions

In higher spatial dimensions both species can coexist and one obtains a phase diagram with two continuous transition lines, which is qualitatively similar to that of the mean-field approximation. The numerically determined phase diagram in 2+1 dimensions is shown in Figure 5. The critical thresholds obtained by varying λ_A/μ agrees with those obtained by varying λ_S/μ, which confirms the correctness of the results. The multicritical point is located at

$$\lambda_A^{(c)}/\mu = 0.41219(1), \quad \lambda_S^{(c)} = 0, \tag{19}$$

where the evolution of species A is critical and branching of S is not allowed. In fact, even for very small $\lambda_S > 0$ species S should be able to survive as species A becomes extinct, eventually approaching $\rho_S = 1$. Therefore, as in mean-field theory, the multicritical point is located exactly at $\lambda_S^{(c)} = 0$.

In order to determine the critical exponents in the stationary state, we performed simulations at several points in the phase diagram close to the phase boundaries. The lattice size was $L^2 = 300 \times 300$ sites. After 200 000 time steps the densities of A and S reached a stationary value. The fluctuations were within 5% of this value. To determine the mean densities, the density was averaged over an additional 100 000 time steps.

For the extinction of species A at the vertical transition line, the expected directed percolation behavior $\rho_A \sim (\lambda_A - \lambda_A^{(c)})^{\beta_A}$ with $\beta_A = \beta_{DP} \simeq 0.583$ is clearly seen in the simulations. However, the evaluation of the critical exponent β_S in the vicinity of the curved phase transition line turned out to be more difficult. For example, close to the multicritical point the estimates were found to depend on the direction in which the line is approached, which is known to be impossible in standard critical phenomena. In fact, reliable estimates could only be obtained far away from the multicritical point. Choosing $\lambda_S/\mu = 60$, where the density of species A is high, and estimating the exponent only in a limited range of the data close to criticality (see Fig. 6), we find numerical evidence that the transition along the curved line belongs to the DP universality class.

Approaching the multicritical point deviations from the expected power law behavior become more pronounced. This is demonstrated in Figure 7, where we measured ρ_S for $\lambda_A/\mu = 1$, approaching the curved transition line vertically from above. To estimate the size of the critical region, the data points for ρ_S were plotted including error bars. Then, a power-law was fitted to the first k data points, with k being small enough to be close to the scaling regime. The measured critical exponent was compatible with $\beta_S = 0.585 \pm 0.05$ everywhere. This confirms that the entire phase transition line (the solid curved line in Fig. 5) except for the multicritical point belongs to the DP universality class.

In order to quantify how the critical behavior is approached we defined critical regions whose size is determined by the requirement that the error bar of the last data point in Figure 7 still touches the power-law fit. The size of these regions with respect to variations of λ_A and λ_S are indicated in Figure 5 by dashed lines. Although their size is arbitrary in the sense that it depends on the chosen accuracy of the computer simulations, it illustrates why estimates far away from the multicritical point are more reliable. Moreover, it is interesting to note that the critical region for variation of λ_A/μ is much larger than the one for λ_S/μ.

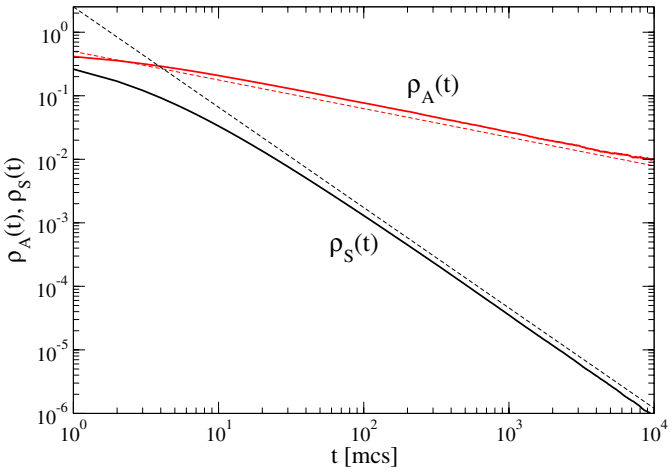

Fig. 8. Decay of the densities $\rho_A(t)$ and $\rho_S(t)$ at the multicritical point in 2+1 dimensions. The dashed line indicate the slopes $-\delta$ and $-\theta$ (see text).

As we approach the multicritical point the critical regions become narrower for both variations. In the immediate vicinity of the multicritical point ($\lambda_A/\mu < 0.5$ and $\lambda_S/\mu < 1$), a reliable estimation of the critical exponent β_S becomes extremely difficult due to huge fluctuations of ρ_S. Here we have an almost instant increase in the density of S as we vary the control parameters. Below, we will determine the shape of the curved phase transition line close to the multicritical point with a better precision by using dynamical simulations.

4.3 Dynamical properties in 2+1 dimensions

In order to compare the time dependence of $\rho_S(t)$ in 2+1 dimensions with the mean field prediction shown in Figure 2, we first performed numerical simulations along the vertical line $\lambda_A = \lambda_A^{(c)}$, where the DP process of species A is critical. Starting with a homogeneous random mixture of both species, we monitor the evolution of the densities $\rho_A(t)$ and $\rho_S(t)$ for various values of λ_S/μ.

The results of simulations *at* the multicritical point $\lambda_A = \lambda_A^{(c)}, \lambda_S = 0$ are shown in Figure 8. As expected, the density of species A decays as

$$\rho_A(t) \sim t^{-\delta}, \tag{20}$$

where $\delta = \beta/\nu_\parallel \approx 0.451$ is the usual decay exponent of DP in two dimensions. Similarly, the density of species S is found to decay algebraically as $\rho_S(t) \sim t^{-\theta}$ with an exponent $\theta \approx 1.6$.

The value of the exponent θ can be explained as follows: initially each site is randomly occupied by A or S with equal probability. As time evolves the critical DP-process of species A gradually removes species S, leading to a monotonous decrease of $\rho_S(t)$. As species S does not create offspring at the multicritical point, all sites occupied by S at time t are precisely those sites that have never been occupied before by species A. Hence $\rho_S(t)$ is the probability that a given site has never been visited by the DP process of species A. In the literature this probability is known as the *local persistence probability* [26] $P_\ell(t)$ of directed percolation. This quantity was shown to decay algebraically as $P_\ell(t) \sim t^{-\theta}$, where θ is the so-called local persistence exponent which seems to be independent of the other DP exponents. In one spatial dimension its value was estimated by $\theta = 1.50(1)$, while in two dimensions we find a slightly higher value $\theta = 1.58(3)$. This observation allows us to conclude that $\rho_S(t)$ decays at the multicritical point as

$$\rho_S(t) \sim t^{-\theta}, \qquad (\epsilon_A = \epsilon_S = 0)\,. \tag{21}$$

Increasing λ_S (while keeping the A-process critical) we allow species S to expand in the voids of the A-process. In this case the algebraic decay (21) is expected to cross over to a growth of surviving S-domains. This density continues to increase until the entire empty space is conquered so that ρ_S approaches the value 1. Our simulation results for this process are shown in the top left panel of Figure 10. Obviously, the temporal behavior of $\rho_S(t)$ resembles the mean field solution in Figure 2, where three different dynamical regimes were identified. However, as an important difference we note that in regime II the density ρ_S increases *algebraically* as t^d in finite-dimensional systems whereas in the mean-field limit the increase is exponential. Consequently, the two crossover time scales between the regimes are expected to scale differently.

Next, we performed numerical simulations on the curved phase transition line. The results are shown in the top right panel of Figure 10. For short times, ρ_S decays again as $t^{-\theta}$, i.e., the difference between the two critical lines is not yet felt. For large times, when ρ_A has become stationary, ρ_S decays as $t^{-\delta}$, i.e., it behaves as a directed percolation process at its critical point. Between these two regimes, there is an increase in the density ρ_S, which is not seen in the mean-field theory. As we will discuss further below, the reason for this is that the characteristic time scales for the cutoff of the initial decay and the onset of the DP decay scale differently with ϵ_S, while there is no distinction between the two scales in mean-field theory. Therefore, in two- or three-dimensional systems the density ρ_S increases in the intermediate regime, where the spreading to empty patches has become relevant, while the critical DP behavior, which requires stationary of ρ_A, is not yet established. In analogy to the behavior on the vertical transition line, we denote the three regimes of initial decay, intermediate increase and ultimate decay with regime I, II, and III.

4.4 Functional form of the curved transition line

In the mean-field case the curved transition line was shown to be a segment of a parabola which terminates at the multicritical point with slope 1 (see Eq. (6)). In low dimensions it is therefore natural to assume a power-law of the form

$$\epsilon_S^* \propto (\epsilon_A^*)^y\,, \tag{22}$$

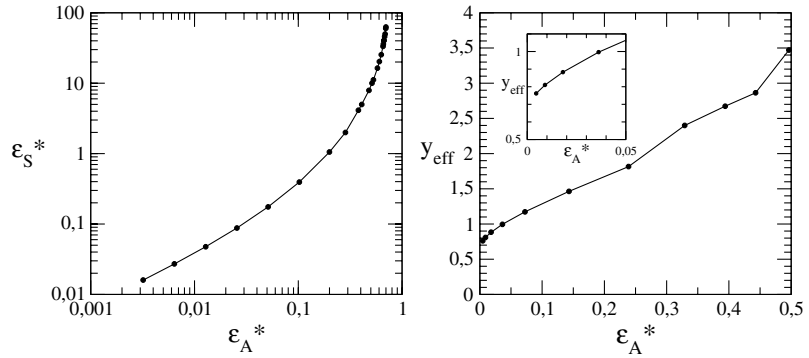

Fig. 9. Left panel: critical line for the extinction of species S for small ϵ_A^* and ϵ_S^*. Right panel: corresponding local slopes for a visual extrapolation. The inset suggests an asymptotic value $y \approx 0.7$.

where again

$$\epsilon_A = \left(\lambda_A - \lambda_A^{(c)}\right)/\mu, \qquad \epsilon_S = \lambda_S/\mu \tag{23}$$

are the reduced parameters and y is an unknown exponent with the mean-field value $y^{\mathrm{MF}} = 1$. As in the mean-field case, this power law may be superposed by next-leading algebraic corrections.

In order to determine the value of the unknown exponent y in 2+1 dimensions numerically, we adjusted the parameters ϵ_A and ϵ_S in such a way that $\rho_S(t)$ decays eventually in the same way as in a DP process. However, the determination of y turns out to be extremely difficult. In particular, the estimates seem to drift to smaller values as we approach the multicritical point. Extrapolating the local slopes (see Fig. 9) we arrive at the conclusion that $y \leq 1$, probably $y \approx 0.7(2)$.

5 Scaling properties

In this section, we interpret the observed results in terms of phenomenological scaling arguments. It turns out that the presence of different scales makes it impossible to formulate a unified scaling theory for the whole dynamical range, instead we find two different scaling forms for regimes I, II and II, III, respectively with a common overlap in region II.

Starting point is the DP-process of species A which decouples from the dynamics of species S. Close to criticality this DP process is known to be invariant under scale transformations

$$\epsilon_A \to \Lambda\epsilon_A, \quad \rho_A \to \Lambda^\beta \rho_A, \quad t \to \Lambda^{-\nu_\parallel} t, \tag{24}$$

where $\Lambda > 0$ is a scaling factor while β and $\nu_\parallel$ are DP exponents listed in Table 1. As usual scale invariance implies that the density is a homogeneous function, i.e.,

$$\rho_A\left(\epsilon_A, t\right) = \Lambda^{-\beta} \rho_A\left(\Lambda\epsilon_A, \Lambda^{-\nu_\parallel} t\right). \tag{25}$$

Setting $\Lambda = t^{1/\nu_\parallel}$ and suppressing non-universal metric factors one obtains the usual scaling form

$$\rho_A(t) = t^{-\delta}\, F_A\left(\epsilon_A t^{1/\nu_\parallel}\right), \tag{26}$$

where F_A is a universal scaling function. In order to derive a similar scaling form for the dynamics of species S in the vicinity of the multicritical point, it is natural to postulate analogous scaling properties for ϵ_S and ρ_S, i.e.

$$\rho_S \to \Lambda^{x_1}\rho_S, \qquad \epsilon_S \to \Lambda^{x_2}\epsilon_S \tag{27}$$

with certain exponents x_1 and x_2. Scale invariance then implies that

$$\rho_S\left(\epsilon_A, \epsilon_S, t\right) = \Lambda^{-x_1}\, \rho_S\left(\Lambda\epsilon_A,\, \Lambda^{x_2}\epsilon_S, \Lambda^{-\nu_\parallel} t\right). \tag{28}$$

Choosing again $\Lambda = t^{1/\nu_\parallel}$ we are led to the scaling form

$$\rho_S\left(\epsilon_A, \epsilon_S, t\right) = t^{-x_1/\nu_\parallel}\, F_S\left(\epsilon_A\, t^{1/\nu_\parallel},\, \epsilon_S\, t^{x_2/\nu_\parallel}\right) \tag{29}$$

where F_S is another scaling function. However, as we will see below, this simple scaling form is not capable to describe the whole dynamical evolution of ρ_s, instead it can be used only partially either in the regimes I, II or in II, III, in each case with a different set of exponents x_1 and x_2. Furthermore, sufficiently close to the curved critical line, the distance from the critical line becomes a relevant parameter, and we will derive a scaling form that uses this variable.

5.1 Crossover between the regimes I and II

In regimes I and II, the decay of ρ_A is yet far from becoming stationary, and the decay of ρ_S should be described by the same expression (29) everywhere near the multicritical point, and in particular on the two critical lines.

In order to determine the exponents x_1 and x_2 in regimes I and II let us first consider the multicritical point $\epsilon_A = \epsilon_S = 0$. Here the scaling form (29) reduces to $\rho_S(t) = t^{-x_1/\nu_\parallel} F_S(0,0)$ which — compared with equation (21) — gives

$$x_1 = \theta\nu_\parallel. \tag{30}$$

Moving up the vertical phase transition line, the DP process of species A remains critical but species S recovers after some time. It is natural to expect that the crossover from decay (regime I) to subsequent growth (regime II) takes place at a typical time scale

$$t_c^{(1)} \sim 1/\epsilon_S \tag{31}$$

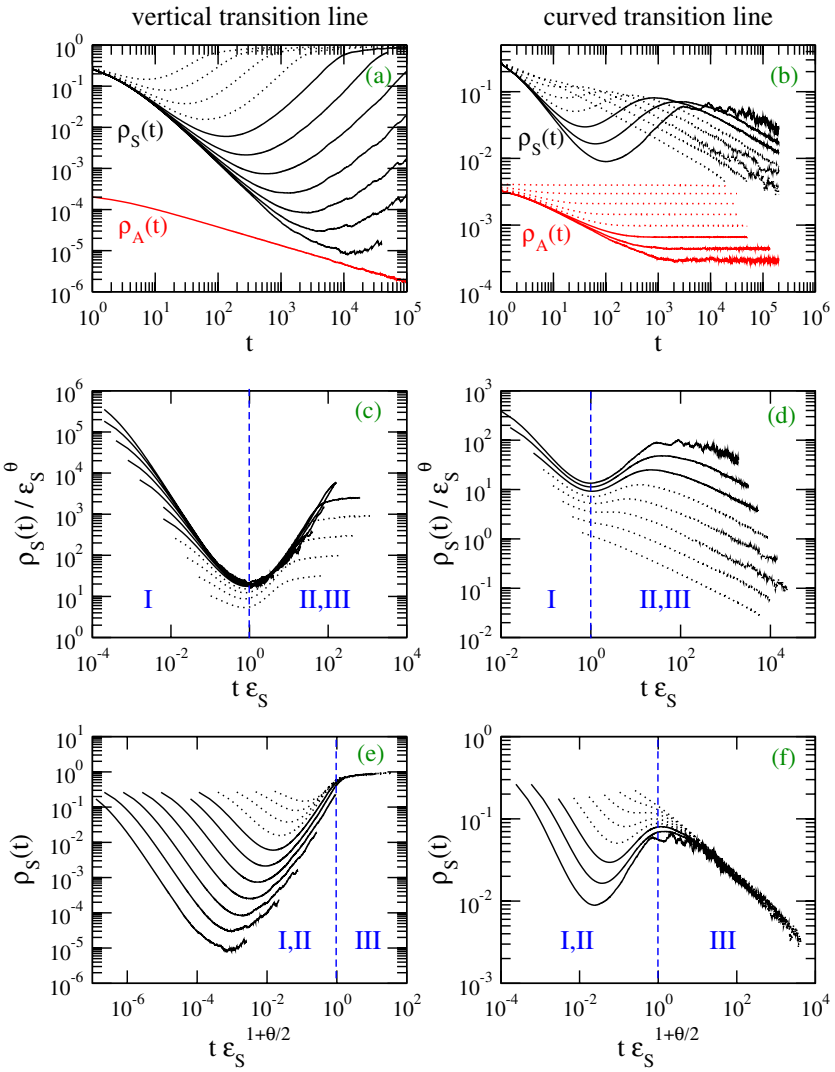

Fig. 10. Simulations in 2+1 dimensions. The left column shows results obtained along the vertical transition line $\epsilon_A = 0$ for $\epsilon_S = 0.0001, 0.0002, \ldots, 0.1024$ while the right column displays similar results taken at the curved phase transition line for $\epsilon_A^* = 0.0016, 0.0032, \ldots, 0.2048$. Data sets far away from the multicritical point ($\epsilon_S \geq 0.0512$), where scaling is poor, are represented as dotted lines. The panels are arranged in three rows. The first row shows the densities $\rho_S(t)$ and $\rho_A(t)$, the latter vertically shifted. In the second row the scaling form (33) is used to collapse the curves in the dynamical regimes I and II (see text). Similarly, the third row shows data collapses based on the scaling form (38) which is valid in the regimes II and III. The respective crossovers are indicated by vertical dashed lines.

which is inversely proportional to the rate of spreading of species S. Scale invariance of the second argument of equation (29) then implies that

$$x_2 = \nu_\parallel. \tag{32}$$

Therefore, we arrive at the scaling form

$$\rho_S\left(\epsilon_A, \epsilon_S, t\right) = t^{-\theta}\, F_S^{(1)}\left(\epsilon_A\, t^{1/\nu_\parallel},\, \epsilon_S t\right). \tag{33}$$

This scaling form can be verified along the vertical line by plotting $\rho_S(t)\epsilon_S^\theta$ versus $t\epsilon_S$ for various values of ϵ_S and checking for a data collapse. As shown in the second row of Figure 10, this data collapse works nicely at the crossover between the dynamical regime I to II (initial decay and subsequent increase) while it clearly fails in regime III.

The first argument of $F_S^{(1)}$ is in fact irrelevant, since the density ρ_S does not depend on it in regimes I and II. However, it will be relevant in regime III, where ρ_A becomes stationary and determines the long-term behavior of ρ_S.

5.2 Crossover between the regimes II and III

The failure of a data collapse in regime III according to equation (33) suggests the presence of two different time scales in the system, namely, a crossover time scale

$$t_c^{(1)} \sim \epsilon_S^{-1} \tag{34}$$

from where on offspring production becomes relevant, and a second time scale $t_c^{(2)}$ from where on species S feels the

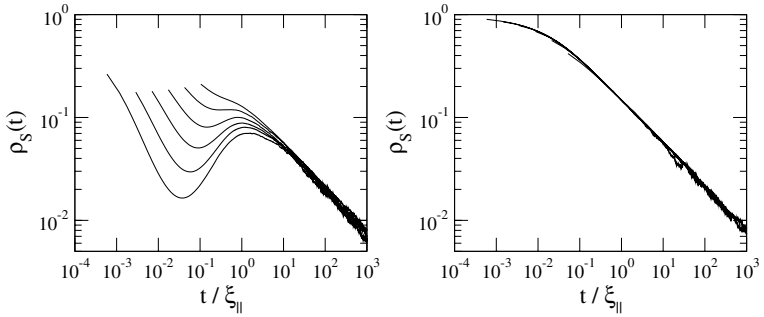

Fig. 11. Left panel: same data as in Figure 10f, but with time measured in units of $\xi_{\|} \sim \epsilon_A^{-\nu_{\|}}$ on the horizontal axis. Right panel: simulation with the same parameters, but with a stationary initial distribution of A particles.

stationary behavior of species A which either induces a critical DP-like decay of species S towards zero on the curved transition line or to an asymptotically stationary value of ρ_S in the coexistence region and on the vertical line. To determine this second crossover time let us first consider the vertical phase transition line, where species A evolves as a critical contact process. After the initial persistence-like decay the remaining S particles are the seeds of d-dimensional spheres growing linearly by offspring production essentially unchallenged by species A. Therefore, in finite dimensions d the density ρ_S increases as t^d. On the vertical phase transition line this growth continues until the density of species S saturates at the value $\rho_S \approx 1$, which defines the second crossover time. Thus, matching initial decay and subsequent growth this second crossover time has to scale as

$$t_c^{(2)} \sim \epsilon_S^{-1-\theta/d}. \tag{35}$$

Therefore, in finite dimensions the two crossover times $t_c^{(1)}$ and $t_c^{(2)}$ scale *differently* with respect to ϵ_S which explains the necessity of two separate scaling forms.

The exponents x_1 and x_2 for the crossover from regime II to regime III can be determined as follows. On the one hand, the density ρ_S saturates at the value 1 for $t \to \infty$ on the vertical phase transition line, independent of ϵ_S, implying that

$$x_1 = 0. \tag{36}$$

On the other hand, scale invariance of the argument of the scaling function in equation (29) requires that

$$x_2 = \frac{\nu_{\|}}{1+\theta/d}. \tag{37}$$

Therefore, the resulting scaling form reads:

$$\rho_S\left(\epsilon_A, \epsilon_S, t\right) = F_S^{(2)}\left(\epsilon_A\, t^{1/\nu_{\|}},\, \epsilon_S t^{1/(1+\theta/d)}\right). \tag{38}$$

This scaling form can be verified numerically by a data collapse along the vertical transition line, as demonstrated in Figure 10e. In Figure 10f we demonstrate that this data collapse works not only at the vertical transition line but also along the curved phase transition line. Since the DP-like decay of ρ_S is expected to set in when ρ_A becomes stationary, i.e., at time $t \sim \epsilon_A^{-\nu_{\|}}$, it follows that the two time scales, namely, the DP correlation time $\xi_{\|} \sim \epsilon_A^{-\nu_{\|}}$ and the second crossover time $t_c^{(2)} \sim \epsilon_S^{-(1+\theta/d)}$ become identical on the curved critical line. More specifically, the phase transition line is expected to be characterized by a constant value of the scale-invariant combination $\epsilon_A^{-\nu_{\|}}/\epsilon_S^{-(1+\theta/d)}$, hence

$$\epsilon_S^* \propto (\epsilon_A^*)^y, \qquad y = x_2 = \frac{\nu_{\|}}{1+\theta/d}. \tag{39}$$

Inserting the numerical estimates $\nu_{\|} = 1.295(6)$ and $\theta = 1.58(3)$ we obtain

$$y = 0.72(1) \tag{40}$$

in fair agreement with the numerically extrapolated value in Section 4.4.

For large times, the expression (38) for ρ_S must approach an asymptotic value that is independent of time. We therefore obtain

$$\lim_{t\to\infty} F_S^{(2)}(z_1, z_2) = \frac{z_2}{z_1^{\epsilon}} \sim \frac{\epsilon_S}{\epsilon_A^y}. \tag{41}$$

This implies that lines of constant density in the ϵ_S-ϵ_A-plane are given by constant ratios ϵ_S/ϵ_A^y.

As we have mentioned, the scaling relation (39) implies that the DP-like decay of species S sets in only after its density has increased to a considerable value. At this time species S has lost the memory of its past, and its dynamics is essentially determined by species A. Therefore, the time evolution $\rho_S(t)$ is from then on identical to the one obtained starting the simulation with a stationary ρ_A and with a finite and random occupation with S. This conclusion is supported by comparing the two simulations, as shown in Figure 11. The range of the axes is the same in both panels, and one can clearly see that for sufficiently large times the two types of curves agree. This agreement of the large-time behavior for the two different types of initial conditions occurs also in the mean-field theory, as mentioned at the end of Section 3.

5.3 Scaling near the curved transition line in regime III

Finally let us study the asymptotic critical behavior of ρ_S in the vicinity of the curved phase transition line. Close

to the multicritical point we have shown that this line can be parametrized by

$$\epsilon_S^* = a(\epsilon_A^*)^y, \tag{42}$$

where a is non-universal metric factor. On the curved line the density $\rho_S(t)$ decays asymptotically as $t^{-\delta}$, i.e., as in a critical DP process. Slightly above in the coexistence phase, $\rho_S(t)$ will eventually saturate at a value proportional to $(\Delta_S)^\beta$, where $\Delta_S = \epsilon_S - \epsilon_S^*$ denotes again the vertical distance from the line. This means that in addition to the previously discussed invariance under the transformation

$$\epsilon_A \to \Lambda\epsilon_A, \quad \epsilon_S \to \Lambda^y\epsilon_S, \quad t \to \Lambda^{-\nu_\parallel}t \tag{43}$$

the system *simultaneously* has to be invariant under the DP-like scale transformation

$$\Delta_S \to \Omega\Delta_S, \quad t \to \Omega^{-\nu_\parallel}t, \quad \rho_S \to \Omega^\beta\rho_S \tag{44}$$

with another scale factor Ω independent of Λ. The second type of scale invariance further constraints the form of $\rho_s(\epsilon_A, \epsilon_S, t)$, effectively reducing the number of independent arguments in the corresponding scaling form to 1. To see this it is convenient to switch from the parameters (ϵ_A, ϵ_S) to the parameters (ϵ_A, δ_S), where

$$\delta_S(\epsilon_A, \epsilon_S) = \frac{\Delta_S}{\epsilon_S^*(\epsilon_A)} = \frac{\epsilon_S}{a\epsilon_A^y} - 1 \tag{45}$$

is the normalized distance from the critical line. In terms of these new parameters, the scaling form (38) is expressed equivalently as

$$\rho_S(\epsilon_A, \delta_S, t) = G_S(\epsilon_A\, t^{1/\nu_\parallel},\, \delta_S), \tag{46}$$

where $G_S(z_1, z_2) = F_S^{(2)}\big(z_1,\, az_1^y(1+z_2)\big)$. Obviously, the parameter δ_S is invariant under the first type of scale transformation (43) while it scales as $\delta_S \to \Omega\delta_S$ under the second type of scale transformations (44). Applying the latter to the scaling form (46) yields

$$\rho_s(\epsilon_A, \delta_S, t) = \Omega^{-\beta}\, G_S(\Omega^{-1}\epsilon_A\, t^{1/\nu_\parallel},\, \Omega\delta_S). \tag{47}$$

Setting $\Omega = \delta_S^{-1}$ one obtains

$$\rho_S(\epsilon_A, \delta_S, t) = \delta_S^\beta\, \tilde{G}_S(\delta_S\, \epsilon_A\, t^{1/\nu_\parallel}). \tag{48}$$

In fact, the argument $\delta_S\, \epsilon_A\, t^{1/\nu_\parallel}$ is a scale-invariant ratio under *both* types of scale transformations, proving that the off-critical DP-process of species A and the almost-critical DP-process of species S can be described in terms of a unified scaling theory. We emphasize that this scaling form is valid *only* in the temporal regime III close to the curved phase transition line, where $\delta_S \ll 1$.

The scaling form (48) reproduces the expected DP behavior. Initially the system does not yet feel the influence of δ_S, hence $\tilde{G}_S(z) \sim z^{-\beta}$ for small z. Later, for $\delta_S > 0$, the initial DP-like decay of ρ_S crosses over to a stationary value, meaning that for large arguments $\tilde{G}_S(z)$ becomes constant. Hence ρ_S evolves as

$$\rho_S(\epsilon_A, \delta_S, t) \sim \begin{cases} (t/\xi_\parallel)^{-\delta} & \text{for} \quad 1 \ll t/\xi_\parallel \ll \delta_S^{-\nu_\parallel} \\ \delta_S^\beta & \text{for} \quad t/\xi_\parallel \gg \delta_S^{-\nu_\parallel}, \end{cases} \tag{49}$$

where $\xi_\parallel \sim \epsilon_A^{-\nu_\parallel}$ is the stationary correlation length of species A.

Exactly on the curved transition line, we have $\delta_S = 0$, and ρ_S therefore decays forever. The unit time is set by $\xi_\parallel$, which is the life time of the largest voids of the A-process. Close to the curved transition line, a decay of ρ_S with $t^{-\delta}$ occurs only if the time scale for saturation, $\xi_\parallel\delta_S^{-\nu_\parallel}$ is larger than the crossover time $t_c^{(2)}$, implying $\Delta_S \ll \epsilon_S$, or, equivalently, $\delta_S \ll 1$. Otherwise, as we have already mentioned, the scaling form (48) is not valid, and saturation sets in directly after the growth in regime II, without DP-like decay of ρ_S.

Finally, let us compare the results once more to mean-field theory. In mean-field theory, the two crossover times scale in the same way, making the distinction between two different scaling forms unnecessary and removing the intermediate growth in regime II close to the critical line, where the DP-like decay of ρ_S becomes visible. The values of the exponents are in mean-field theory $\beta = y = \theta = \nu_\parallel = 1$. The behavior in regime III near the critical line that we found in mean-field theory resembles qualitatively the one described in this section. In particular, the proportionality factor between ρ_S and Δ_S diverges at the multicritical point, and so does the factor in front of the $t^{-\delta}$ decay.

6 Conclusions

In this paper we have introduced a simple model of two competing species A and S feeding on the same resources and living in "patches" represented by lattice sites. Species A is characterized by fast reproduction and can therefore displace species S and evolves independently according to the dynamic rules of a contact process. Hence it belongs to the universality class of directed percolation. Special S has a lower reproduction rate and is therefore restricted to live in those patches where A is absent. In contrast to species A, which can die out in a patch, patches occupied by species S do not become empty spontaneously.

In one spatial dimension, the phase diagram comprises two different phases where one of the species goes extinct, separated by a first-order transition line. In higher dimensions an additional mixed phase emerges, bounded by two continuous transition lines. This mixed phase is characterized by a non-trivial coexistence of the two species in the stationary state[1].

[1] We note that by increasing the width of the one-dimensional system from one lattice site to several lattice sites (e.g. a strip of $2 \times L$ sites), one can generate a modified version of the model where the two species can coexist even in one dimension, and where the phase transition of S is also continuous.

The curved phase transition line (except for the multicritical point) is found to belong to the DP universality class. This result may be surprising because S-individuals do not vanish spontaneously. On the other hand the result is also plausible since species S 'percolates' in the voids of the *supercritical* DP of species A. Since the spatio-temporal arrangement of species A involves only short-range correlations these voids are uncorrelated on large scales, which effectively leads to a DP transition.

At the multicritical point the correlation lengths of the A-process diverges, leading to a non-trivial scaling behavior. In this case, starting with a mixed random initial conditions, S-occupied patches mark those lattice sites that have been never visited by a species A before. Therefore, the density ρ_S decays in the same way as the so-called local persistence probability in DP. For $\lambda_S > 0$, however, this decay crosses over to an increase of ρ_S when the reproduction of S becomes visible. This increase continues until a stationary state is reached in which the two species coexist if the parameters are not too close to the curved phase transition line. Close to the curved phase transition line, ρ_S decreases again after times long enough that ρ_A has become stationary and saturates eventually at a small nonzero value depending on the distance to the critical line. We succeeded in introducing scaling variables and scaling functions that characterize the behavior of ρ_S in the different regimes.

References

1. J. Marro, R. Dickman, *Nonequilibrium phase transitions in lattice models* (Cambridge University Press, Cambridge, 1999)
2. W. Kinzel, Z. Phys. B **58**, 229 (1985)
3. H. Hinrichsen, Adv. Phys. **49**, 815 (2000)
4. G. Ódor, Rev. Mod. Phys. **76**, 663 (2004)
5. S. Lübeck, Int. J. Mod. Phys. B **18**, 3977 (2004)
6. H.K. Janssen, Z. Phys. B **42**, 151 (1981)
7. P. Grassberger, Z. Phys. B **47**, 365 (1982)
8. H.-K. Janssen, U.C. Täuber, Ann. Phys. (NY) **315**, 147 (2005)
9. R.M. Ziff, E. Gulari, Y. Barshad, Phys. Rev. Lett. **56**, 2553 (1986)
10. G. Grinstein, Z.W. Lai, D.A. Browne, Phys. Rev. A **40**, 4820 (1989)
11. I. Jensen, H.C. Fogedby, R. Dickman, Phys. Rev. A **41**, 3411 (1990)
12. I. Jensen, Phys. Rev. Lett. **70**, 1465 (1993)
13. M.A. Muñoz, G. Grinstein, R. Dickman, R. Livi, Phys. Rev. Lett. **76**, 451 (1996)
14. U.C. Täuber, M.J. Howard, H. Hinrichsen, Phys. Rev. Lett. **80**, 2165 (1998)
15. Y.Y. Goldschmidt, H. Hinrichsen, M.J. Howard, U.C. Täuber, Phys. Rev. E **59**, 6381 (1999)
16. K.E. Bassler, D.A. Browne, Phys. Rev. Lett. **77**, 4094 (1996)
17. L. Canet, H. Chaté, B. Delamotte, Phys. Rev. Lett. **92**, 255703 (2004)
18. D. Tilman, P. Karveia, *Spatial Ecology: The Role of Space in Popolation Dynamics and Inter-specific Interactions* (Princeton University Press, Princeton USA, 1997)
19. S.C. Palmer, R.A. Norton, Biochemical systematics and ecology **20**, 219 (1992)
20. I. Schön, R.K. Butlin, H.I. Griffiths, K. Martens, Proc. R. Soc. Lond. B **265**, 235 (1997)
21. H.J. Muller, Mut. Res. **1**, 29 (1964)
22. T.E. Harris, Ann. Prob. **2**, 969 (1974)
23. I. Jensen, R. Dickman, J. Stat. Phys. **71**, 89 (1993)
24. R. Dickman, Phys. Rev. E **60**, 2441 (1999)
25. S. Lübeck, R.D. Willmann, Nuclear Physics B **718**, 341 (2005); S. Lübeck, Int. J. Mod. Phys. B **18**, 3977 (2004)
26. H. Hinrichsen, H.M. Koduvely, Eur. Phys. J. B **5**, 257 (1998)